IOPscience iopscience.iop.org

Home Search Collections Journals About Contact us My IOPscience

Locking-free finite element formulation for steel-concrete composite members

This article has been downloaded from IOPscience. Please scroll down to see the full text article.

2010 IOP Conf. Ser.: Mater. Sci. Eng. 10 012239

(http://iopscience.iop.org/1757-899X/10/1/012239)

View the table of contents for this issue, or go to the journal homepage for more

Download details:
IP Address: 138.25.51.66
The article was downloaded on 01/09/2010 at 02:41

Please note that terms and conditions apply.

Locking-free Finite Element Formulation for Steel-Concrete Composite Members

R Emre Erkmen[1] and Mark A Bradford[2]
[1] Centre for Infrastructure Engineering and Safety, School of Civil and Environmental Engineering, The University of New South Wales, Sydney, NSW 2052, Australia.

[2] Faculty of Engineering, University of Technology, Sydney P.O. Box123, Broadway, NSW 2007, Australia.

E-mail: emre.erkmen@unsw.edu.au

Abstract. In the conventional displacement-based finite element analysis of composite beam-columns that consist of two Euler-Bernoulli beams juxtaposed with a deformable shear connection, the coupling of the transverse and longitudinal displacement fields may cause oscillations in interlayer slip field and reduction in optimal convergence rate, known as slip-locking. This locking phenomenon is typical of multi-field problems of this type, and is known to produce erroneous results for the displacement based finite element analysis of composite beam-columns based on cubic transverse and linear longitudinal interpolation fields. In this paper it will be shown that by simple change of the pair of dependent variables in the formulation the locking behaviour can be alleviated. An example is presented to illustrate the effects of connection stiffness on the behaviour of composite beams and the results show that the proposed approach is efficient in alleviating the locking behaviour.

1. Introduction

Composite beams-columns are structural members formed when two beams are connected by means of shear connectors to form an interacting unit that is capable of resisting bending moments and axial forces. The simplest composite beam model with flexible shear connectors was initially developed by Newmark et al. [1], in which two Euler-Bernoulli beams are connected by assuming that vertical separation does not occur between the components. Subsequently, several displacement-based finite element formulations were developed based on Newmark's model. These include those of Arizumi et al. [2], Daniels and Crisinel [3], Ranzi et al. [4, 5] and Dall'Asta and Zona [6]. However, displacement-based finite element formulations may suffer from the so-called slip-locking phenomenon because of the coupling between the displacement fields [7]. In order to overcome the limitations of many displacement-based finite element formulations, mixed and force-based finite element formulations were suggested by Salari et al. [8], Ayoub and Filippou [9], Ayoub [10], and Dall'Asta and Zona [11]. On the other hand, the consistent interpolation strategy has been employed by Dall'Asta and Zona [12], and Ranzi and Zona [13] to develop locking-free displacement-based finite element formulations for composite beam-columns. In this paper we are alleviating the locking

[1] To whom any correspondence should be addressed.

© 2010 Published under licence by IOP Publishing Ltd

behaviour by a simple change of the conventional primary variables in the composite beam-column formulation. An example is presented to illustrate the effects of connection stiffness on the behaviour of composite beams. Numerical results presented illustrate the efficiency of the proposed formulation.

2. Composite beam-column analysis

2.1. Displacements and strains

The basic kinematic assumptions adopted in this paper were initially presented by Newmark et al. [1] based on which the composite member is composed of a top and a bottom Euler-Bernoulli beam elements, which are referred to as beams 1 and 2 as shown in Figure 1(a). The composite cross-section is thus represented as $A=A_1+A_2$, where A_1 and A_2 are the cross-sections of beams 1 and 2, respectively. The displacement field adopted in the formulation consists of the vertical displacement v of the selected reference axis, and the longitudinal displacements w_1 and w_2 of the centroids of beams 1 and 2, respectively as shown in Figure 1(b). The slip at the interface between the two components of the composite beam is Γ, as shown in Figure 1(b), which is due to the difference in longitudinal displacements w_1 and w_2, and the rotation of both cross-sections v', i.e.

$$\Gamma = w_2 - w_1 + hv' , \tag{1}$$

where h is the distance between the centroids of the beams, and $(\ )' = d(\ )/dz$. Strain expressions in each component can be determined by using the Euler-Bernoulli beam kinematics, hence in terms of the extensions w_1' and w_2' and the curvature v'' due to bending deformations as

$$\varepsilon_1 = w_1' - (y - h_1)v'' , \tag{2}$$

$$\varepsilon_2 = w_2' - (y - h_2)v'' , \tag{3}$$

where h_1 and h_2 are the coordinates of the centroids of beams 1 and 2 with respect to the reference axis, respectively as shown in Figure 1(c).

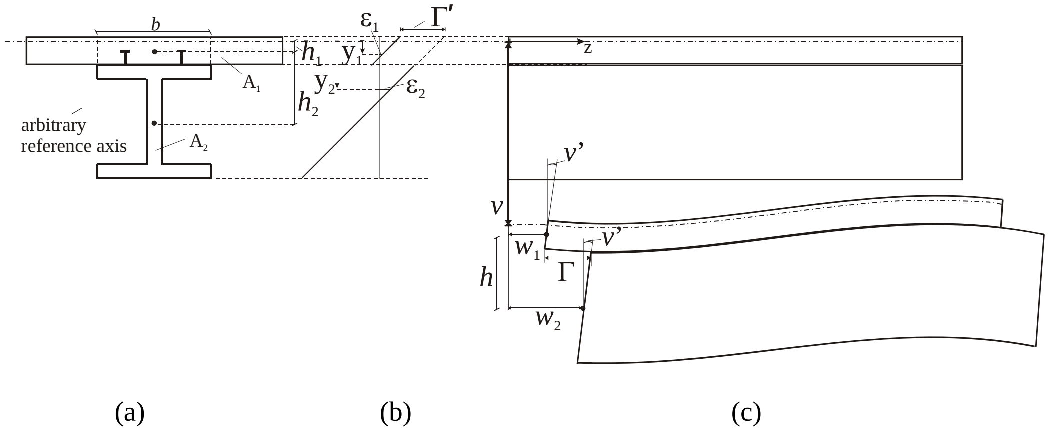

Figure 1. Composite beam-column; (a) cross-section, (b) strains, (c) displacements.

3. Finite element formulations

3.1. Basic displacement based finite element formulation
A displacement based finite element formulation can be developed by employing the total potential energy functional, i.e.

$$\Pi = \tfrac{1}{2}\int_L\int_{A_1} E_1\varepsilon_1^2 \mathrm{d}A\mathrm{d}z + \tfrac{1}{2}\int_L\int_{A_2} E_2\varepsilon_2^2 \mathrm{d}A\mathrm{d}z + \tfrac{1}{2}\int_L\int_b \rho\Gamma^2 \mathrm{d}x\mathrm{d}z - \Pi_{ext}\,, \tag{4}$$

where the first and second integrals are the elastic bending energies of the two Euler-Bernoulli beam components, the third integral is due to the elastic deformations of the shear connection in which ρ is its elastic stiffness (force/length^3) which is the shear stress in longitudinal direction per unit slip, b is the width of the effective interface surface between the two beam components, and Π_{ext} is the work done by the external forces. In a displacement-based finite element formulation, the longitudinal displacement fields w_1 and w_2 and the derivative of the vertical displacement field v' can be expressed in terms of the selected interpolation functions as

$$\begin{Bmatrix} w_1 \\ w_2 \\ v' \end{Bmatrix} = \begin{bmatrix} \mathbf{M}(z) & \mathbf{0} & \mathbf{0} \\ \mathbf{0} & \mathbf{M}(z) & \mathbf{0} \\ \mathbf{0} & \mathbf{0} & \mathbf{N}'(z) \end{bmatrix} \begin{Bmatrix} \mathbf{w}_{N1} \\ \mathbf{w}_{N2} \\ \mathbf{v}_N \end{Bmatrix} = \mathbf{B}(z)\mathbf{U}\,, \tag{5}$$

where $\mathbf{M}(z)$ and $\mathbf{N}(z)$ are the vectors of the interpolation functions for the longitudinal and the vertical displacement fields respectively. In Equation (5), $\mathbf{B}(z)$ is the discrete interlayer slip matrix and $\mathbf{U}$ is the vector of nodal displacements composed of the vectors of nodal longitudinal displacements at the centroids of both beams $\mathbf{w}_{N1}$, $\mathbf{w}_{N2}$ and the vertical displacement $\mathbf{v}_N$, i.e.

$$\mathbf{U}^{\mathrm{T}} = \left\langle \mathbf{w}_{N1}^{\mathrm{T}} \quad \mathbf{w}_{N2}^{\mathrm{T}} \quad \mathbf{v}_N^{\mathrm{T}} \right\rangle . \tag{6}$$

By using Equations (1) to (3) and (5) in Equation (4), the total potential energy functional can be written as

$$\Pi = \tfrac{1}{2}\mathbf{U}^{\mathrm{T}}\left(\int_L \mathbf{B}_d^{\mathrm{T}}(z)\mathbf{D}\mathbf{B}_d(z)\mathrm{d}z\right)\mathbf{U} + \tfrac{1}{2}\mathbf{U}^{\mathrm{T}}\left(\int_L \mathbf{B}^{\mathrm{T}}(z)\mathbf{D}_\rho\mathbf{B}(z)\mathrm{d}z\right)\mathbf{U} - \mathbf{F}\mathbf{U}\,, \tag{7}$$

in which $\mathbf{B}_d(z) = \mathbf{B}'(z)$, $\mathbf{F}$ is the energy equivalent nodal external load vector,

$$\mathbf{D} = \begin{bmatrix} E_1A_1 & 0 & 0 \\ 0 & E_2A_2 & 0 \\ 0 & 0 & E_1I_1 + E_2I_2 \end{bmatrix}, \tag{8}$$

and

$$\mathbf{D}_{\boldsymbol{\rho}} = \rho b \begin{bmatrix} 1 & -1 & -h \\ -1 & 1 & h \\ -h & h & h^2 \end{bmatrix}, \tag{9}$$

where I_1 and I_2 are the second moments of area of the beams with respect to their horizontal principal axes passing through the centroids of each cross-section and $h = h_2 - h_1$. From the first variation of the total potential energy functional, the weak form of the equilibrium equations are obtained as

$$\left(\mathbf{K}_b + \mathbf{K}_s\right)\mathbf{U} = \mathbf{F}, \tag{10}$$

where $\mathbf{K}_b$ is the stiffness matrix associated with the bending and the axial deformations of the beam components and $\mathbf{K}_s$ is associated with the slip energy i.e.

$$\mathbf{K}_b = \int_L \mathbf{B}_d^{\mathrm{T}}(z)\mathbf{D}\mathbf{B}_d(z)\mathrm{d}z, \tag{11}$$

$$\mathbf{K}_s = \int_L \mathbf{B}^{\mathrm{T}}(z)\mathbf{D}_\rho\mathbf{B}(z)\mathrm{d}z. \tag{12}$$

The simplest element that satisfies the compatibility conditions can be developed by using linear interpolations for the longitudinal displacements and cubic interpolation for the vertical displacement, i.e.

$$\mathbf{M}(z) = \left\langle \left(1 - z/L\right) \quad z/L \right\rangle, \tag{13}$$

$$\mathbf{N}(z) = \left\langle \left(1 - \frac{3z^2}{L^2} + \frac{2z^3}{L^3}\right) \quad \left(z - \frac{2z^2}{L} + \frac{z^3}{L^2}\right) \quad \left(\frac{3z^2}{L^2} - \frac{2z^3}{L^3}\right) \quad \left(-\frac{z^2}{L} + \frac{z^3}{L^2}\right) \right\rangle \tag{14}$$

and the vector of nodal displacement $\mathbf{U}$ can be written as

$$\mathbf{U}^{\mathrm{T}} = \left\langle w_1(0) \quad w_1(L) \quad w_2(0) \quad w_2(L) \quad v(0) \quad v'(0) \quad v(L) \quad v'(L) \right\rangle. \tag{15}$$

This element will be referred as the Basic Element (BE) herein. It has been reported that for stiff shear connection, i.e. for the limit case of $\rho \to \infty$, BE suffers from slip-locking (e.g., Dall'Asta and Zona [7]). The cause of locking in BE can be seen by substituting Equations (13) to (15) into Equation (1) to obtain the discretized form of the interlayer slip Γ as

$$\Gamma = \Gamma(0)\left(1 - \frac{z}{L}\right) + \Gamma(L)\frac{z}{L} + c\frac{6h}{L^2}\left(z - \frac{z^2}{L}\right), \tag{16}$$

where $\Gamma(0)$ and $\Gamma(L)$ are nodal slip values, i.e.

$$\Gamma(0) = w_2(0) - w_1(0) + hv'(0), \tag{17}$$

$$\Gamma(L) = w_2(L) - w_1(L) + hv'(L). \tag{18}$$

In Equation (16), constant c can be written as

$$c = v(L) - v(0) - \frac{L}{2}\left[v'(L) + v'(0)\right], \tag{19}$$

which is non-zero unless the vertical displacement field v is parabolic rather than cubic. The condition $\Gamma = 0$ for the limit case of $\rho \to \infty$, causes Equation (19) to vanish which enforces a constant value for the curvature v'', thus for stiffer connection stiffness ρ the convergence rate of BE reduces. On the other hand, *c* is not zero in general therefore constant slip cannot be produced by using Equation (16) and that causes oscillations in the slip field.

3.2. Finite element formulation based on the change of primary variables

By changing the primary variables of the formulation from the axial displacements of the both components at the centroids and the vertical displacement of the axis to the vertical and axial displacements of the arbitrary reference axis *v* and *w*, respectively and the slip at the intersection Γ, the longitudinal strain expressions can be written as

$$\varepsilon_1 = w' - yv'' - \Gamma', \tag{20}$$

$$\varepsilon_2 = w' - yv''. \tag{21}$$

From Equations (20) and (21) and using the vector of changed nodal displacements, i.e., $\mathbf{V}^{\mathrm{T}} = \left\langle \mathbf{w}_N^{\mathrm{T}} \quad \mathbf{v}_N^{\mathrm{T}} \quad \mathbf{\Gamma}_N^{\mathrm{T}} \right\rangle$, the longitudinal strains can be written as

$$\varepsilon_1 = \langle 1 \quad -y \rangle \begin{bmatrix} \mathbf{N}'(z) & \mathbf{0} & \mathbf{M}'(z) \\ \mathbf{0} & \mathbf{M}''(z) & \mathbf{0} \end{bmatrix} \begin{Bmatrix} \mathbf{w}_N \\ \mathbf{v}_N \\ \mathbf{\Gamma}_N \end{Bmatrix} = \langle 1 \quad -y \rangle \overline{\mathbf{B}}_1(z)\mathbf{V}, \tag{22}$$

$$\varepsilon_2 = \langle 1 \quad -y \rangle \begin{bmatrix} \mathbf{N}'(z) & \mathbf{0} & \mathbf{0} \\ \mathbf{0} & \mathbf{M}''(z) & \mathbf{0} \end{bmatrix} \begin{Bmatrix} \mathbf{w}_N \\ \mathbf{v}_N \\ \mathbf{\Gamma}_N \end{Bmatrix} = \langle 1 \quad -y \rangle \overline{\mathbf{B}}_2(z)\mathbf{V}. \tag{23}$$

By substituting Equations (22), (23) into Equation (4), the total potential energy functional can be written as

$$\Pi = \tfrac{1}{2}\mathbf{V}^{\mathrm{T}}\int_L \overline{\mathbf{B}}_1^{\mathrm{T}}(z)\mathbf{D}_1\overline{\mathbf{B}}_1(z)\mathrm{d}z\mathbf{V} + \tfrac{1}{2}\mathbf{V}^{\mathrm{T}}\int_L \overline{\mathbf{B}}_2^{\mathrm{T}}(z)\mathbf{D}_2\overline{\mathbf{B}}_2(z)\mathrm{d}z\mathbf{V} + \tfrac{1}{2}\mathbf{V}^{\mathrm{T}}\int_L \mathbf{B}_\rho^{\mathrm{T}}(z)^{\mathrm{T}}\rho b\mathbf{B}_\rho(z)\mathrm{d}z\mathbf{V} - \mathbf{F}\mathbf{V}, \tag{24}$$

in which

$$\mathbf{B}_\rho(z) = \begin{bmatrix} \mathbf{0} & \mathbf{0} & \mathbf{0} \\ \mathbf{0} & \mathbf{0} & \mathbf{0} \\ \mathbf{0} & \mathbf{0} & \mathbf{M}'(z) \end{bmatrix}, \tag{25}$$

and

$$\mathbf{D}_1 = E_1\begin{bmatrix} A_1 & -S_{x1} \\ -S_{x1} & I_{x1} \end{bmatrix}, \tag{26}$$

$$\mathbf{D}_2 = E_2 \begin{bmatrix} A_2 & -S_{x2} \\ -S_{x2} & I_{x2} \end{bmatrix}, \tag{27}$$

where S_{x1}, I_{x1}, S_{x2} and I_{x2} are the first and second moments of area of each component of the beam with respect to the selected reference axis. From the first variation of the total potential energy functional, the weak form of the equilibrium equations can be obtained as

$$\left(\bar{\mathbf{K}}_1 + \bar{\mathbf{K}}_2 + \bar{\mathbf{K}}_\rho\right)\mathbf{V} = \mathbf{F}, \tag{28}$$

where $\bar{\mathbf{K}}_1$ and $\bar{\mathbf{K}}_2$ are the stiffness matrices associated with the bending and the axial deformations of the beam components and $\bar{\mathbf{K}}_\rho$ is associated with the slip energy i.e.

$$\bar{\mathbf{K}}_1 = \int_L \bar{\mathbf{B}}_1^{\mathrm{T}}(z)\mathbf{D}_1\bar{\mathbf{B}}_1(z)\mathrm{d}z, \tag{29}$$

$$\bar{\mathbf{K}}_2 = \int_L \bar{\mathbf{B}}_2^{\mathrm{T}}(z)\mathbf{D}_2\bar{\mathbf{B}}_2(z)\mathrm{d}z, \tag{30}$$

$$\bar{\mathbf{K}}_\rho = \int_L \mathbf{B}_\rho^{\mathrm{T}}(z)^{\mathrm{T}}\rho b\mathbf{B}_\rho(z)\mathrm{d}z. \tag{31}$$

In the limit case of $\rho \to \infty$, no oscillations occur in the slip field since $\Gamma = 0$ does not impose any constraints other than $\Gamma(0) = 0$ and $\Gamma(L) = 0$ as opposed to the conventional displacement based FE formulation BE in Section 3 in which zero slip condition imposes a constant value for the curvature v''. Thus due to proposed change of variables pure Euler-Bernoulli beam-column behaviour can be captured for both steel and concrete components as shown in Figure 2, i.e. $\varepsilon_1 = \varepsilon_2 = w' - yv''$.

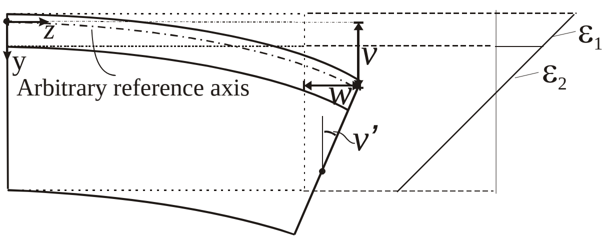

Figure 2. Euler-Bernoulli mode of deformation

4. Application

The evidence of locking behaviour for the basic element (BE) and the performances of the proposed element (PE) is discussed on a simply supported beam which is subjected to 1kN/m vertical uniform distributed load. The total span of the beam is L=10 m in all cases. The top component of the cross-section has a modulus of elasticity of E_1=200×10^3 MPa. The width and the thickness of this rectangular top section (Figure 1(a)) is B_d =400mm and t_d = 15mm respectively. The modulus of elasticity of the bottom component is E_2=26×10^3 MPa. The overall height, flange width, flange thickness and web thickness of the bottom I-section are D_g = 312mm, B_g = 200mm, t_f =12 mm and

t_w=8 mm respectively. The beam axis is selected at the centroid of the bottom component. Analyses were undertaken for two different connection stiffness parameters ρ=0.1N/mm^3 (αL=3.5) and ρ=100N/mm^3 (αL=110.9) and the results are compared with the exact solutions. The effective intersection surface width between the two components is b=150mm which is used in the dimensionless connection stiffness parameter, i.e. $\alpha=\sqrt{\rho b\left[1/(E_1A_1)+1/(E_2A_2)+h^2/(E_1I_1+E_2I_2)\right]}$. Figure 3 shows the vertical deflection, slip and curvatures based on four element solutions, respectively based on which it can be shown that BE depicts stiffer behaviour then the exact solution when the connection stiffness is increased (Fig. 3.b). Also, slip oscillations start to occur (Fig. 3.d) and the curvature within the element tends to be constant values when the connection stiffness is increased (Fig. 3.f). On the other hand PE's performance is not affected by the connection stiffness and the results are closed to the exact solution. In order to illustrate the convergence performance the analyses were made for one, two and four element models.

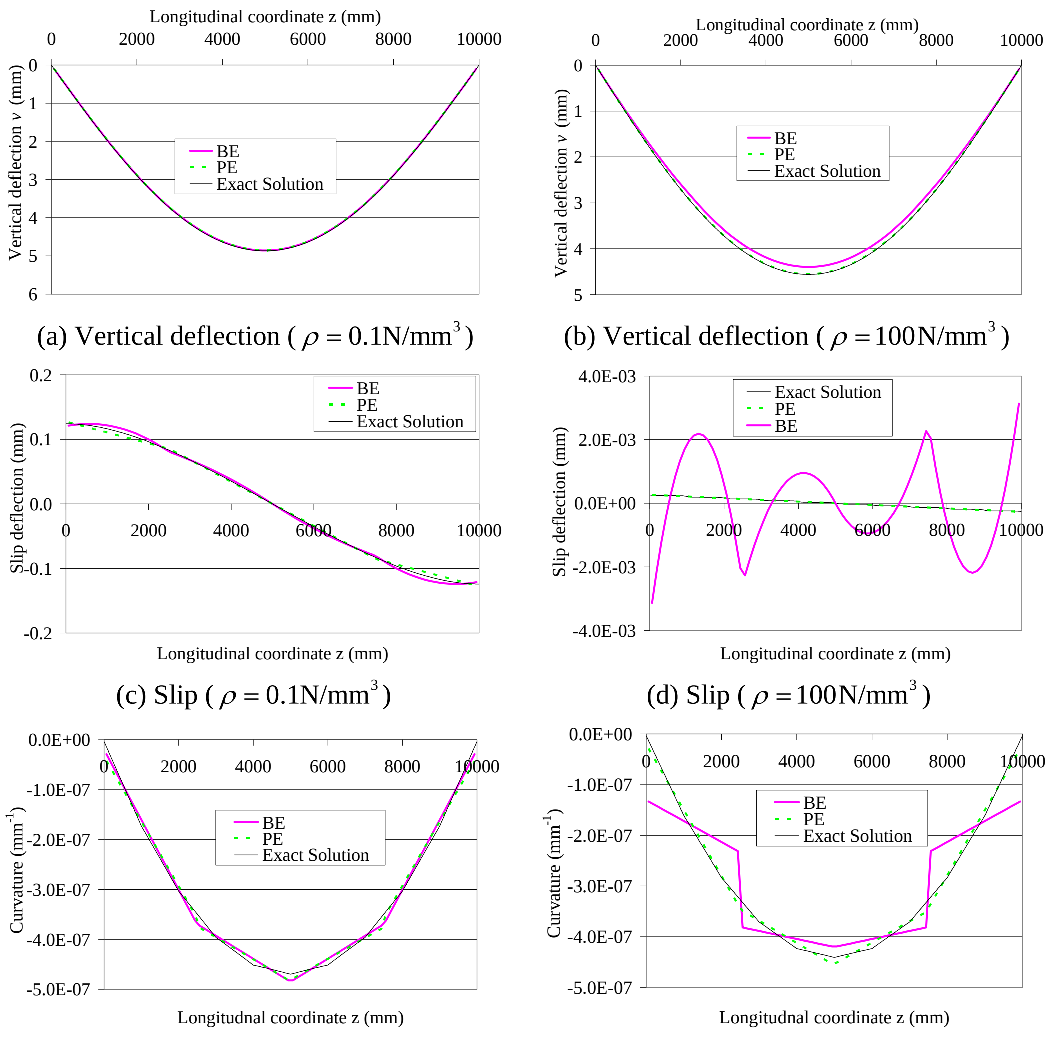

(a) Vertical deflection ($\rho=0.1\text{N/mm}^3$) (b) Vertical deflection ($\rho=100\text{N/mm}^3$)

(c) Slip ($\rho=0.1\text{N/mm}^3$) (d) Slip ($\rho=100\text{N/mm}^3$)

(e) Curvature ($\rho=0.1\text{N/mm}^3$) (f) Curvature ($\rho=100\text{N/mm}^3$)

Figure 3. Analysis results for the simply supported beam

The convergence performances of the elements based on the total strain energy are shown in Figures 4 (a) and (b) which illustrates that when the connection stiffness increases BE suffers from poor convergence rate due to slip-locking where PE's performance is not effected by the increment in connection stiffness.

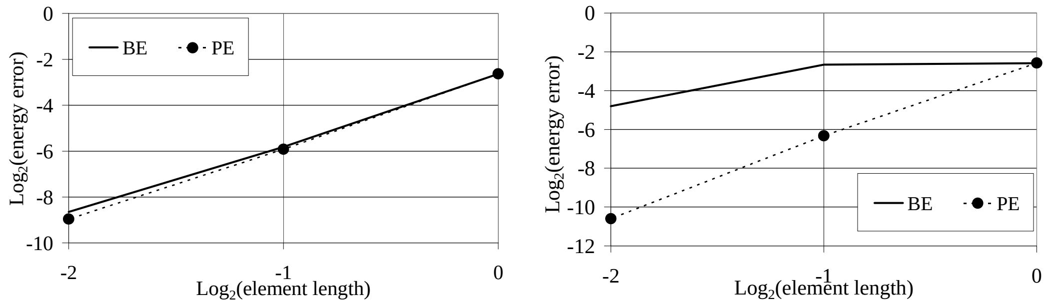

(a) Convergence rate ($\rho = 0.1\text{N/mm}^3$) (b) Convergence rate ($\rho = 100\text{N/mm}^3$)

Figure 4. Accuracy and convergence rate for the simply supported beam

Figure 5 shows that the error in the energy norm for BE increases when the dimensionless stiffness parameter is increased however the energy error in the results based PE solution even decreases when the stiffness parameter increases. Thus, PE does not suffer from the slip-locking.

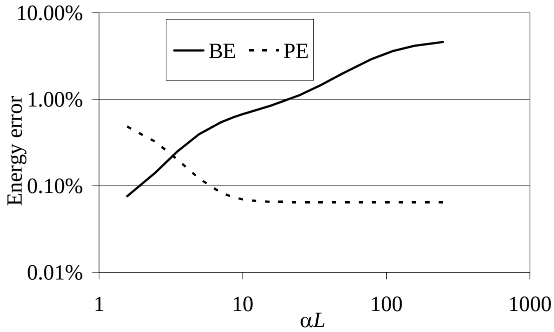

Figure 5. Energy error versus connection stiffness based on four elements

5. Conclusions

The displacement based finite element formulation based on the linear interpolation of the longitudinal displacement fields of the components and the cubic interpolation of the vertical displacement field suffers from locking when used for the analysis of composite beam-columns consist of two Euler-Bernoulli beams juxtaposed with a deformable shear connection. The main problem with the conventional displacement based formulation is that for stiff connections the nodal values of slip may be totally erroneous and severe oscillations occur in the slip field. The basic displacement finite element formulation also suffers from degradation in accuracy and convergence rate when the connection stiffness is increased. In this study the displacement based finite element formulation was modified by changing the dependent variables in the variational formulation which alleviates the oscillations due to locking and significantly improves the accuracy and convergence characteristics. The selected example verifies that the proposed approach is accurate and efficient.

References

[1] Newmark NM, Siess CP and Viest IM 1951. Tests and analysis of composite beams with incomplete interaction. *Proc. Soc. Exp. Stress Anal.* **9**(1) 75-92.

[2] Arizumi Y, Yamada S and Kajita T 1981. Elastic-plastic analysis of composite beams with incomplete interaction by finite element method. *Comp. Struct.* **14** 543-462

[3] Daniels B and Crisinel M 1993. Composite slab behaviour and strength analysis. Part I: Calculation procedure. *J. Struct. Engrg.* ASCE **119**(1) 16-35.

[4] Ranzi G, Bradford MA and Uy B 2004. A direct stiffness analysis of a composite beam with partial interaction. *Int. J. Num. Meth. Engrg* **61**(5) 657-672.

[5] Ranzi G and Bradford MA 2009. Analysis of composite beams with partial interaction using the direct stiffness approach accounting for time effects. *International Journal for Numerical Methods in Engineering* **78**(5) 564-586.

[6] Dall'Asta, A and Zona A 2002. Non-linear analysis of composite beams by a displacement approach. *Comp. Struct.* **80** 2217-2228.

[7] Ranzi G, Gara F, Leoni G and Bradford MA 2006. Analysis of composite beams with partial shear interaction using available modelling techniques: A comparative study. *Comp. Struct.* **84** 930-941.

[8] Salari MR, Spacone E, Shing PB and Frangopol DM 1998. Nonlinear analysis of composite beams with deformable shear connectors. *J. Struct. Engrg.* ASCE **124**(10) 1148-1158.

[9] Ayoub A and Filippou FC 2000. Mixed formulation of nonlinear steel-concrete composite beam elements. *J. Struct. Engrg* ASCE **126**(3) 371-381.

[10] Ayoub A 2005. A force-based model for composite steel-concrete beams with partial interaction. *J. Constr. Steel Res.* **61** 387-414.

[11] Dall'Asta A and Zona A 2004. Three-field mixed formulation for non-linear analysis of composite beams with deformable shear connection. *Fin. Elem. Anal. Des.* **40**(4):425-448.

[12] Dall'Asta A and Zona A 2004. Slip locking in finite elements for composite beams with deformable shear connection. *Fin. Elem. Anal. Des.* **40**:1907-1930.

[13] Ranzi G and Zona A 2007. A steel–concrete composite beam model with partial interaction including the shear deformability of the steel component. *Engrg. Struc*. **29**(11) 3026-3041.

IOPscience iopscience.iop.org

Home Search Collections Journals About Contact us My IOPscience

9th World Congress on Computational Mechanics and 4th Asian Pacific Congress on Computational Mechanics

This article has been downloaded from IOPscience. Please scroll down to see the full text article.

2010 IOP Conf. Ser.: Mater. Sci. Eng. 10 011001

(http://iopscience.iop.org/1757-899X/10/1/011001)

View the table of contents for this issue, or go to the journal homepage for more

Download details:
IP Address: 138.25.51.66
The article was downloaded on 01/09/2010 at 02:13

Please note that terms and conditions apply.

IOP Conf. Series: Materials Science and Engineering **10** (2010) 011001 doi:10.1088/1757-899X/10/1/011001

Preface

The use for mathematical models of natural phenomena has underpinned science and engineering for centuries, but until the advent of modern computers and computational methods, the full utility of most of these models remained outside the reach of the engineering communities. Since World War II, advances in computational methods have transformed the way engineering and science is undertaken throughout the world. Today, theories of mechanics of solids and fluids, electromagnetism, heat transfer, plasma physics, and other scientific disciplines are implemented through computational methods in engineering analysis, design, manufacturing, and in studying broad classes of physical phenomena. The discipline concerned with the application of computational methods is now a key area of research, education, and application throughout the world.

In the early 1980's, the International Association for Computational Mechanics (IACM) was founded to promote activities related to computational mechanics and has made impressive progress. The most important scientific event of IACM is the World Congress on Computational Mechanics. The first was held in Austin (USA) in 1986 and then in Stuttgart (Germany) in 1990, Chiba (Japan) in 1994, Buenos Aires (Argentina) in 1998, Vienna (Austria) in 2002, Beijing (China) in 2004, Los Angeles (USA) in 2006 and Venice (Italy) in 2008. The 9th World Congress on Computational Mechanics is held in conjunction with the 4th Asian Pacific Congress on Computational Mechanics under the auspices of Australian Association for Computational Mechanics (AACM), Asian Pacific Association for Computational Mechanics (APACM) and International Association for Computational Mechanics (IACM).

The 1st Asian Pacific Congress was in Sydney (Australia) in 2001, then in Beijing (China) in 2004 and Kyoto (Japan) in 2007.

The WCCM/APCOM 2010 publications consist of a printed book of abstracts given to delegates, along with 247 full length peer reviewed papers published with free access online in IOP Conference Series: Materials Science and Engineering. The editors acknowledge the help of the paper reviewers in maintaining a high standard of assessment and the co-operation of the authors in complying with the requirements of the editors and the reviewers.

We also would like to take this opportunity to thank the members of the Local Organising Committee and the International Scientific Committee for helping make WCCM/APCOM 2010 a successful event. We also thank The University of New South Wales, The University of Newcastle, the Centre for Infrastructure Engineering and Safety (CIES), IACM, APCAM, AACM for their financial support, along with the United States Association for Computational Mechanics for the Travel Awards made available.

N Khalili
S Valliappan
Q Li
A Russell
19 July 2010
Sydney, Australia

© 2010 Published under licence by IOP Publishing Ltd